Journal of Applied Electrochemistry (2007) 37:311–314
DOI 10.1007/s10800-006-9241-9

Phase structure and electrochemical properties of $Ml_{1-x}Mg_xNi_{2.78}Co_{0.50}Mn_{0.11}Al_{0.11}$ hydrogen storage alloys

Z. ZHANG[1,3], S. M. HAN[1,2,*], W. GUAN[2], Y. LI[2], Y. W. LIU[2], Q. TONG[2] and T. F. JING[1,3]
[1]*State Key Laboratory of Metastable Materials Science and Technology, Qinhuangdao, 066004, P.R. China*
[2]*Department of Environmental and Chemical Engineering, Yanshan University, Qinhuangdao, 066004, P.R. China*
[3]*Department of Material Science and Engineering, Yanshan University, Qinhuangdao, 066004, P.R. China*
*(*author for correspondence, fax: +86-335-8061569, e-mail: hanshm@ysu.edu.cn)*

Received 3 April 2006; accepted in revised form 11 September 2006

Key words: electrochemical properties, hydrogen storage alloys, magnesium content, MH/Ni battery, phase structure

Abstract

The effect of magnesium content on the phase structure and electrochemical properties of $Ml_{1-x}Mg_xNi_{2.78}Co_{0.50}Mn_{0.11}Al_{0.11}$ (x = 0.05, 0.10, 0.20, 0.30) hydrogen storage alloys was investigated. The results of X-ray diffraction reveal that all the alloys consist of the major phase (La, Mg)Ni_3 and the secondary phase $LaNi_5$. With increase in x, the relative content of the (La, Mg)Ni_3 phase increases gradually, and the maximum capacity and low temperature dischargeability of the alloy electrodes first increase and then decrease. When x is 0.20, the discharge capacity of the alloy electrode reaches 363 mAh g^{-1} at 293 K and 216 mAh g^{-1} at 233 K, respectively. The high rate dischargeability of the alloy electrodes increases with increase in x. When the discharge current density is 1200 mA g^{-1}, the high rate dischargeability of the alloy electrodes increases from 22.0% to 50.4% with x increasing from 0.05 to 0.30. The cycling stability of the electrodes decreases gradually with increase in magnesium content.

1. Introduction

Due to the high specific energy and environmental friendliness, MH/Ni batteries using hydrogen storage alloy as negative material have been widely investigated and applied in portable computers, cellular telephones, new cordless appliances and hybrid electric vehicles [1–3]. Among all the developed hydrogen storage alloys, rare earth-based AB_5 type alloys have been industrialized, but their discharge capacity, low temperature dischargeability and high rate dischargeability are not satisfactory. Therefore, developing a novel type of hydrogen storage alloy with higher hydrogen storage capacity and better overall electrochemical properties is very urgent. In recent years, a new type R–Mg–Ni-based AB_3-type (R = rare earth, Ca or Y) hydrogen storage alloys with high hydrogen storage capacity have been studied [4–7], which brought a new development opportunity for MH/Ni batteries. In view of their higher electrochemical capacity, La–Mg–Ni-based alloys are considered a promising candidate for the negative electrode material of MH/Ni batteries. La–Mg–$(NiCo)_x$ (x = 3–3.5) quaternary alloys have been investigated by Kohno et al. [8], and the results indicated that the discharge capacity of the $La_{0.70}Mg_{0.30}Ni_{2.80}Co_{0.50}$ alloy reaches 410 mAh g^{-1}, much higher than that of commercially used AB_5-type alloys. Pan et al. [9] studied the structure and electrochemical properties of $La_{0.70}Mg_{0.30}(Ni_{0.85}Co_{0.15})_x$ (x = 2.5–5.0) alloys, and found that the alloy with x = 3.5 had a maximum discharge capacity of 395.6 mAh g^{-1}. Although La–Mg–Ni-based alloys have higher discharge capacity, the cycling stability needs further improvement. It is confirmed that fundamental reasons for the capacity decay of the alloy are the oxidation and pulverization of the alloy during charge/discharge cycling [10]. La and Mg form oxides in alkaline electrolyte, which causes the electrode to lose activity [11]. On the other hand, the lattice internal stress and cell volume expansion, which are inevitable when hydrogen atoms enter the interstices of the lattice, are the real driving force that leads to the pulverization of the alloy [10]. With the object of delaying cycle life degradation, Liu and Pan et al. [12–14] studied the effect of multi-component alloying in the B-sites on cycling stability and other electrochemical properties of new type La–Mg–Ni-based alloys, and found that the presence of Al, Mn and Co is beneficial to improving the cycling stability. However, the cycling stability did not satisfy the need for practical application.

To improve the cycling stability and other properties of R–Mg–Ni-based hydrogen storage alloys, we have used Ml (Ml stands for lanthanum-rich misch-metal) instead of pure elemental La in the A-sites and multi-

component alloying in the B-sites simultaneously to prepare new types of Ml–Mg–Ni(Co–Mn–Al)-based hydrogen storage alloys $Ml_{1-x}Mg_xNi_{2.78}Co_{0.50}Mn_{0.11}Al_{0.11}$ (x = 0.05, 0.10, 0.20, 0.30). The effects of variable Mg content on the phase structure and electrochemical properties of Ml–Mg–Ni(Co–Mn–Al)-based hydrogen storage alloys have been studied systematically.

2. Experimental

$Ml_{1-x}Mg_xNi_{2.78}Co_{0.50}Mn_{0.11}Al_{0.11}$ (x = 0.05, 0.10, 0.20, 0.30) hydrogen storage alloys were prepared by the induction melting under argon atmosphere. The Ml was composed of 69.18 wt.% La, 21.86 wt.% Ce, 2.25 wt.% Pr, and 6.21 wt.% Nd and 0.5 wt.% impurity. The purity of other metals used was higher than 99.9%. A slight excess of Mg was added in order to compensate for evaporative loss during preparation process. The ingots were annealed at 1173 K for 6 h, and burnished the parts of oxidation at surface by sand paper, then mechanically pulverized and ground into fine powers with an average size of 200–300 mesh for the electrochemical measurements and less than 300 mesh for the X-ray diffraction measurements.

Metal hydride electrodes were prepared by uniformly mixing 0.15 g of alloy powders with 0.75 g carbonyl nickel powders, and then cold pressing into pellets about $\Phi 10 \times 1.2$ mm under a pressure of 20 MPa.

The electrochemical measurements were performed at 293 K (except for low temperature measurement) in a half-cell consisting of a working electrode (MH electrode) and sintered $Ni(OH)_2$/NiOOH counter electrode with 6 M KOH solution as the electrolyte. When the discharge capacity, activation and cycling stability of the electrodes were tested, each electrode was charged at 60 mA g^{-1} for 10 h followed by a 10-min break and then discharged at the same current. In investigating the high rate dischargeability (HRD), discharge capacity at 60 mA g^{-1}, 300 mA g^{-1}, 600 mA g^{-1}, 900 mA g^{-1}, 1200 mA g^{-1}, 1500 mA g^{-1} discharge current densities were measured. The electrochemical properties under low temperature were measured after constant temperature for 4 h in an auto constant low temperature equipment ($\pm$1 K). In all the discharge process, the electrodes were discharged to the cut-off voltage of 1.000V.

The XRD patterns of the hydrogen storage alloys were obtained on a D/Max-2500/PC X-ray diffractometer (Cu Kα radiation) and analyzed by Jade-5.0 software.

3. Results and discussion

3.1. *Phase structures*

Figure 1 shows the XRD patterns of $Ml_{1-x}Mg_xNi_{2.78}Co_{0.50}Mn_{0.11}Al_{0.11}$ (x = 0.05, 0.10, 0.20, 0.30) hydrogen storage alloys. It can be seen that

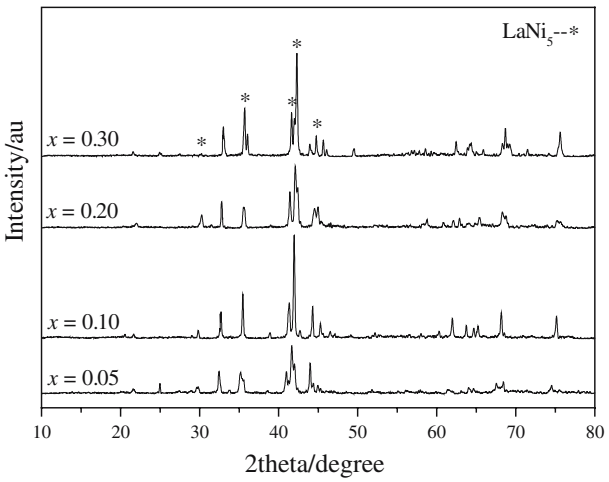

Fig. 1. XRD patterns of $Ml_{1-x}Mg_xNi_{2.78}Co_{0.50}Mn_{0.11}Al_{0.11}$ alloy electrodes.

the major phase of all the alloys is (La, Mg)Ni_3 phase with the rhombohedral $PuNi_3$-type structure, and the other peaks are corresponding to $LaNi_5$ phase with the hexagonal $CaCu_5$-type structure. With increase in x, the intensity of (La, Mg)Ni_3 diffraction peaks increases gradually. This indicates that the relative content of (La, Mg)Ni_3 phase increases and the relative content of $LaNi_5$ phase decreases accordingly. Some studies have indicated that, for the B/A stoichiometric ratio between 3.0 and 4.0, the presence of Mg in the A-site of the rare earth-based hydrogen storage alloys is beneficial to formation of the (La, Mg)Ni_3 phase. [14, 15]

The lattice parameters and cell volume of (La, Mg)Ni_3 phase in $Ml_{1-x}Mg_xNi_{2.78}Co_{0.50}Mn_{0.11}Al_{0.11}$ (x = 0.05, 0.10, 0.20, 0.30) hydrogen storage alloys are listed in Table 1. The increase in x of the alloys leads to a decrease of both lattice constants and cell volume due to the atomic radius of Mg (1.72 Å) being smaller than those of rare earth elements (2.64–2.74 Å).

3.2. *Maximum discharge capacity*

Figure 2 shows the discharge capacity of $Ml_{1-x}Mg_xNi_{2.78}Co_{0.50}Mn_{0.11}Al_{0.11}$ (x = 0.05, 0.10, 0.20, 0.30) alloy electrodes. It can be seen that all these electrodes can be easily activated to reach the maximum discharge capacity within three cycles. The good activation property is meritorious for practical applications. For the alloy electrodes with the composition range of x = 0.05–0.30, the maximum discharge capacity of the

Table 1. Lattice parameters and cell volume of the (La, Mg)Ni_3 phase in $Ml_{1-x}Mg_xNi_{2.78}Co_{0.50}Mn_{0.11}Al_{0.11}$ alloy electrodes

Samples	Lattice parameters		Cell volume/Å^3
	a/Å	c/Å	
X = 0.05	5.090	25.012	561.20
X = 0.10	5.086	25.004	560.14
X = 0.20	5.081	24.976	558.41
X = 0.30	5.069	24.961	555.44

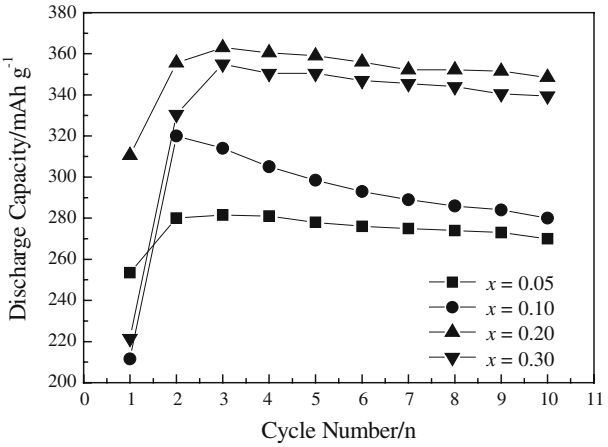

Fig. 2. The relationship between discharge capacity and cycle number of $Ml_{1-x}Mg_xNi_{2.78}Co_{0.50}Mn_{0.11}Al_{0.11}$ alloy electrodes.

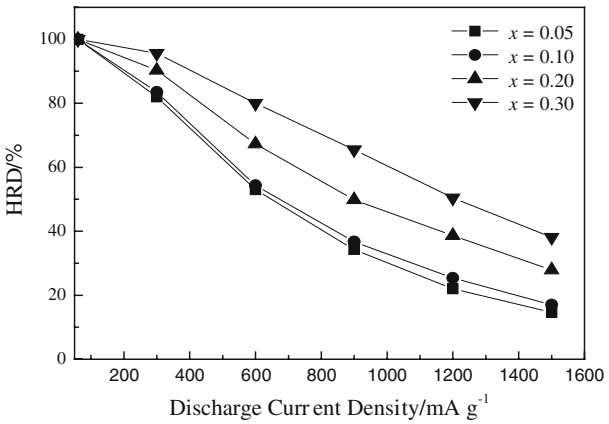

Fig. 3. HRD of the $Ml_{1-x}Mg_xNi_{2.78}Co_{0.50}Mn_{0.11}Al_{0.11}$ alloy electrodes.

alloy electrodes first increases and then decreases as x increases. The $Ml_{0.80}Mg_{0.20}Ni_{2.78}Co_{0.50}Mn_{0.11}Al_{0.11}$ alloy electrode shows the maximum discharge capacity of 363 mAh g^{-1}, which is above 10% higher than that of the commercialized AB_5-type alloys. It has been reported that the hydrogen storage capacity of the $LaNi_3$ phase exceeded that of the well-known hydrogen absorber $LaNi_5$ phase [16]. So with the (La, Mg)Ni_3 phase increasing in the alloys, the maximum discharge capacity also increases. However, with increase in x, the decrease of discharge capacity can be mainly attributed to the variation of the relative content between the (La, Mg)Ni_3 phase and the $LaNi_5$ phase in the alloys, which leads to the decrease of the hydrogen absorption/desorption efficiency of the (La, Mg)Ni_3 phase. The $LaNi_5$ phase has high ability of catalysis, which improves the hydrogen absorption/desorption efficiency of the (La, Mg)Ni_3 phase in the hydrogen adsorption/desorption process. With the relative content of the $LaNi_5$ phase decreasing, the catalysis decrease, which leads to slow hydrogen absorption/desorption efficiency and, therefore, the discharge capacity of the alloy electrode decreases with increase in x from 0.20 to 0.30.

3.3. *High rate dischargeability*

The high rate dischargeability (HRD) is defined and calculated according to the following formula:

$$\mathrm{HRD}(\%) = \frac{C_d}{C_d + C_{60}} \times 100\% \qquad (1)$$

where C_d is the discharge capacity of the electrode discharged at the current density I_d to the cut-off voltage of 1.000 V, C_{60} is the residual discharge capacity at the discharge current density 60 mA g^{-1} to the same cut-off voltage after the alloy electrode has been discharged at the discharge current I_d. Figure 3 shows HRD of the $Ml_{1-x}Mg_xNi_{2.78}Co_{0.50}Mn_{0.11}Al_{0.11}$ (x = 0.05, 0.10, 0.20, 0.30) alloy electrodes. It can be obviously seen that increase in x makes for a better HRD. When the discharge current density is up to 1200 mA g^{-1}, the HRD of the alloy electrodes increases from 22.0% to 50.4% with x increasing from 0.05 to 0.30. This is attributable to the acceleration of the dehydriding process with increasing the Mg content [17].

3.4. *Low temperature dischargeability*

Hydrogen storage alloys used as negative electrode material of MH/Ni batteries are expected to be capable of working over a wider temperature range, especially at low temperature. Figure 4 shows the discharge capacity of $Ml_{1-x}Mg_xNi_{2.78}Co_{0.50}Mn_{0.11}Al_{0.11}$ (x = 0.05, 0.10, 0.20, 0.30) alloy electrodes at temperatures from 233 K to 293 K. The discharge capacity of the alloy electrodes first increases and then decreases with increase in x, but the degree of decrease is different. At 233 K, the discharge capacity is up to 216 mAh g^{-1} when x is 0.20, but those of the other alloy electrodes are less than 100 mAh g^{-1}.

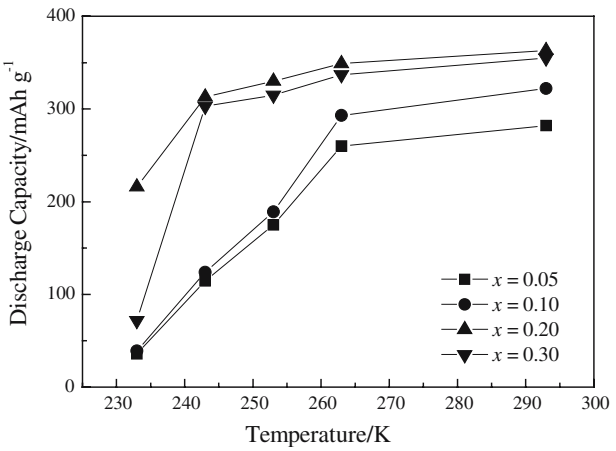

Fig. 4. Discharge capacity of $Ml_{1-x}Mg_xNi_{2.78}Co_{0.50}Mn_{0.11}Al_{0.11}$ alloy electrodes at low temperature.

Table 2. Capacity retention of $Ml_{1-x}Mg_xNi_{2.78}Co_{0.50}Mn_{0.11}Al_{0.11}$ alloy electrodes

Cycle number	Capacity retention, S_n/%			
	$x = 0.05$	$x = 0.10$	$x = 0.20$	$x = 0.30$
100th	82.6	80.2	79.8	76.1
200th	72.7	69.1	68.5	67.0

3.5. *Cycle life*

The capacity retention of the $Ml_{1-x}Mg_xNi_{2.78}Co_{0.50}Mn_{0.11}Al_{0.11}$ ($x = 0.05, 0.10, 0.20, 0.30$) alloy electrodes is shown in Table 2. In order to express the cycling stability, the capacity retention (S_n) is defined as follows:

$$S_n = C_n / C_{max} \times 100\% \quad (2)$$

where C_n is the discharge capacity of the electrode at the nth cycle and C_{max} is the maximum discharge capacity of the alloy electrode. The capacity retention of alloy electrodes decreases gradually with increase in Mg content. When x is 0.05, the capacity retentionremains 82.6% after 100 cycles, which is much higher than that reported by Liao et al. [18](66.7%).The cycling stabilityhas been improved significantly by using Ml instead of pure elemental La. The capacity retention degradation can be mainly attributed to that the corrosion of Mg in alkaline solution and the formation of a permeable $Mg(OH)_2$ passive film which is a very loose gel-type film and offers little protection to the alloy from further corrosion [19]. This leads to an increased rate of contact of the fresh alloy surface with electrolyte and, consequently, a higher rate of corrosion and a more rapid capacity decay [18]. Thus increase in Mg content is deleterious to the cycling stability.

4. Conclusions

(1). The major phase of $Ml_{1-x}Mg_xNi_{2.78}Co_{0.50}Mn_{0.11}Al_{0.11}$ ($x = 0.05, 0.10, 0.20, 0.30$) alloys is (La, Mg)$Ni_3$ phase, and the secondary phase is $LaNi_5$ phase. The relative content of the (La, Mg)Ni_3 phase increases gradually as x increases.

(2). The maximum discharge capacity and low temperature dischargeability of the alloy electrodes both first increase and then decrease with increase in x. When x is 0.20, the discharge capacity of the alloy electrode is up to 363 mAh g^{-1} at 293 K and 216 mAh g^{-1} at 233 K, respectively.

(3) With increase in x, the HRD of the alloy electrodes increases. At the discharge current density of 1200 mA g^{-1}, the HRD of the alloy electrodes increases from 22.0% to 50.4% as x increases from 0.05 to 0.30.

(4) Increase in Mg content induces poor cycle life due to corrosion of Mg in alkaline solution.

Acknowledgement

This work was supported by The National Natural Science Foundation of China (20673093).

References

1. P Gifford, J Adams, D Corrigan and S Venkatesan, *J. Power Sources* **80** (1999) 157.
2. F Haschka, W Warthmann and G Benczru-Urmossy, *J. Power Sources* **72** (1998) 32.
3. X.B. Zhang, Y.J. Chai, W.Y. Yin and M.S. Zhao, *J. Solid State Chem.* **177** (2004) 2373.
4. K Kadir, N Kuriyama, T Sakai, I Uehara and L Eriksson, *J. Alloys Comp.* **284** (1999) 145.
5. K Kadir, T Sakai and I Uehara, *J. Alloys Comp.* **302** (2000) 112.
6. J Chen, H.T. Takeshita, H Tanaka, N Kuriyama, T Sakai, I Uehara and M Haruta, *J. Alloys Comp.* **302** (2000) 304.
7. M Latroche and A Percheron-Guegan, *J. Alloys Comp.* **356**(357) (2003) 461.
8. T Kohno, H Yoshida, F Kawashima, T Inaba, I Sakai, M Yamamoto and M Kanda, *J. Alloys Comp.* **311** (2000) L5.
9. H.G. Pan, Y.F. Liu, M.X. Gao, Y.Q. Lei and Q.D. Wang, *J. Electrochem. Soc.* **150** (2003) A565.
10. Y.H. Zhang, G.Q. Wang, X.P. Dong, S.H. Guo, J.M. Wu and X.L. Wang, *J. Alloys Comp.* **379** (2004) 298.
11. W Guan, S.M. Han, Y Li, M Li, L.R. Mao and L Hu, *J. Chin. Rare Earth Soc.* **23** (2005) 101.
12. Y.F. Liu, H.G. Pan, M.X. Gao, Y.F. Zhu, Y.Q. Lei and Q.D. Wang, *Int. J. Hydrogen Energy* **29** (2004) 297.
13. Y.F. Liu, H.G. Pan, M.X. Gao, R Li, X.Z. Sun and Y.Q. Lei, *J. Alloys Comp.* **388** (2005) 109.
14. H.G. Pan, Y.F. Liu, M.X. Gao, Y.Q. Lei and Q.D. Wang, *J. Electrochem. Soc.* **152** (2005) A326.
15. H.G. Pan, Y.F. Liu, M.X. Gao, Y.F. Zhu, Y.Q. Lei and Q.D. Wang, *J. Alloys Comp.* **351** (2003) 228.
16. H.G. Pan, Y.F. Liu, M.X. Gao, Y.F. Zhu and Y.Q. Lei, *Int. J. Hydrogen Energy* **28** (2003) 219.
17. T Rui, Y.N. Liu, C.C. Zhu, J.W. Zhu and G Yu, *Mater. Chem. Phys.* **95** (2006) 130.
18. B Liao, Y.Q. Lei, L.X. Chen, G.L. Lu, H.G. Pan and Q.D. Wang, *J. Power Sources* **129** (2004) 358.
19. Y Zhang, L.X. Chen, Y.Q. Lei and Q.D. Wang, *Int. J. Hydrogen Energy* **27** (2002) 501.